Development and Evaluation of Automated System for RFID Tag Performance Measurements

Pavel STASA, Jiri SVUB, Filip BENES

Institute of Economics and Control Systems, Faculty of Mining and Geology, VSB–Technical University of Ostrava, 17. listopadu 15/2172, Ostrava, Czech Republic

pavel.stasa@vsb.cz, jiri.svub@vsb.cz, filip.benes@vsb.cz

DOI: 10.15598/aeee.v15i4.2365

Abstract. *The paper discusses the development of a device for directional characteristics measurements of RFID tags marked objects. Current procedures for carrying out laboratory tests of UHF RFID devices rely on relatively high involvement of human labour associated with higher risk of measurements errors. The newly developed system that performs great part of manual operations autonomously reduces the risk of measurement errors and enables experiments to be performed faster, more accurate and in repeatable manner.*

Keywords

Automated system, directional characteristics, RFID measurement chamber, RFID tag, software.

1. Introduction

A typical example of current innovative industrial solutions is the onset of the IoT (Internet of Things), and gradual penetration of the so-called Industry 4.0 in various fields. Hand in hand with this trend comes increasing demand for applications of automatic identification technologies, especially of the RFID (Radio Frequency Identification) technology.

The logical consequence of these trends is also rising interest in identification process quality measurement and testing in the particular field. Perhaps the greatest interest in the new technologies in our region can be seen in the automotive industry where attention is paid to the implementation of lean manufacturing, errors reduction, and application of new technologies to improve production processes.

Nevertheless, the performance of UHF RFID strictly depends on the power emitted by the reader, the tag sensitivity, and the gain and sensitivity of reader. Moreover, the application environments have strong effects on the performance of the passive UHF RFID system [1].

RFID technology is increasingly emphasized in European framework programs (such as Horizon 2020, etc.), as well as at the national level (S3 strategy). Successful and efficient deployment of RFID technology requires careful analysis and design of new systems together with proper measurements and verification of the experiments before introducing it into practice. Thanks to cost reduction of the RFID system and maturity of the IoT technology, the RFID and IoT related industries are growing up and the associated applications are becoming popular [2]. Given the need for clear and distinct interpretation of results through advanced visualization methods the RFID labs often demand the system which takes care of both measurement and processing of the measured results to the desired form.

At our department, we are engaged in research and applications associated with automatic identification technologies and their implementation in practice. To meet the needs of R&D institutions and industrial companies, it was decided to develop our own anechoic chamber for performing higher quality and more accurate testing to support the applications of RFID technology.

To further facilitate the testing process our own custom software has been developed. The software fully automates the measurement process and provides the results in a comprehensive and clear form. The unique combination of designed hardware and software can adjust the analysed object in predefined steps, with the resolution of one degree angle, and it can perform measurements of signal strength required to obtain a response from the tag under test in any position. The RF performance of the RFID system is highly sensitive to its operation environments, tag arrangements, reader and tag designs. The test system utilizes a RFID reader as the air interface to access the RFID tags to provide similar measurement environments used in commercial application systems [2].

Thanks to the complex design of the shielded chamber equipped with electromagnetic radiation absorbing material we are able to eliminate interference with surrounding radiation sources as well as with the inner reflections thus ensuring repeatability with provable unaffected results. For example, Betta et al. proved in their study [3] that the Wi-Fi transmitter can have significant influence on the metrological performance of some instruments, particularly for low distances from the disturbance source (less than 5 m). In addition, the automation of performed tests eliminates influence of human error in the measurements.

2. Related Work

The automated test environments and methods suitable for UHF RFID tag performance are key elements for antenna design, impedance characteristics as well as for choosing right RFID tag for given purposes.

There are several commercially available measurement systems. Among them, the LabVIEW-controlled PXI RF platform by National Instruments [4] can be mentioned. The process of tag test and measurement system is described in paper LabVIEW-Based UHF RFID Tag Test and Measurement System [5]. The Voyantic Tagformance Lite tool [6] is another commercial available measurement system which work as enhanced RFID readers with variable frequency and power and with controllable protocol settings. These systems are extremely accurate but cost several tens of thousands of dollars.

Many scientific contributions were written regarding RFID tag performance measuring and an anechoic chamber was used as a test environment. Among them, Nikitin et al. presented an overview of UHF RFID tag performance characterization [7].

Lee at al. presented solutions for investigation of the properties of RFID tags in an anechoic chamber with a commercially available reader Impinj. Their solution was based on a 3D rendering of RFID system directional characteristics. Our solution uses only one axis of rotation and renders 2D graphs which is sufficient for most applications [2].

Colella et al. [8] presented an accurate and cost-effective measurement platform for the performance analysis of UHF passive RFID tags. It is based on a commercial multiprogrammable UHF RFID reader provided with GPIO ports and controlling a stepper motor. In this way, it can perform the measurement of the minimum emitted power capable to turn ON the tag under test when varying the angle between reader antenna and tag itself. Based on a rigorous theoretical formulation, tag sensitivity, working range, and radiation pattern can be automatically derived. The system guarantees high versatility, since the tag performance can be completely evaluated by varying, besides angle and frequency, also protocol parameters, and interrogation power [8].

The main and important difference between their approach [8] and our system lies in fact that their tests are performed in open space while our solution uses anechoic chamber. Their system [8] is composed of a hardware subsystem and a software subsystem. Process starts from the evaluation of the minimum power emitted by the reader in correspondence of which the tag is activated. The whole system is able to evaluate all the metrics characterizing an RFID tag in the 865–928 MHz bandwidth, also when varying the orientation between tag and reader antenna in steps as small as 1.8°. The system has been validated through the comparison with the Voyantic TagFormance Lite tool, and through the characterization of a specifically designed built-in-lab RFID tag used as testing sample. They presented very good accordance among obtained results confirms the appropriateness of this platform also in the case of sensitivity evaluation [8].

Accurate tag range measurement can be conducted in a controlled environment, such as anechoic chamber or Transverse ElectroMagnetic (TEM) cell. For both methods, tag position can be fixed and transmitter output power can be varied by controlled attenuation. This allows one to carry accurate tag range characterization and avoid using large and prohibitively expensive chambers or cells. Compact TEM cell is a convenient tool for measuring small tags while larger anechoic chamber can be used to measure tag performance on various objects [9].

Another paper shows the technical difference of RFID UHF tags when applied in different kind of materials in a controlled environment, the tests were performed in an anechoic chamber [10]. Additionally, comparison between UHF RFID Tag performance tests realized in two different RF environments is presented in [11]. Both papers show promising results compared to commercial solutions.

Similar approach was described by Felix et al. in [12]. They presented an alternative method to automate RFID tag tests using the tool LabView to control an RFID reader Sirit IN510 and a step motor drive.

The purpose of this paper is to describe the development of automated system for measuring RFID tag performance, especially theirs directional characteristics.

3. Theoretical Background

3.1. Basic Principle and Purpose of Anechoic Chamber

Ensuring measurement repeatability of the so-called directional characteristics of RFID tags is practically impossible in normal conditions. During each measurement, the interference can occur, i.e. a phenomenon in which the moving waves at a certain point reinforce each other, while at other points they cancel each other. This greatly influences the results of measurement and so it is difficult to achieve the same results when repeating experiments.

The ideal and probably the only solution is measurement in the anechoic chamber. It is an electromagnetically shielded space of required dimensions whose inner walls are also lined with electromagnetically absorbent material which strongly reduces internal reflections in the chamber in a wide frequency band [13].

For this is the reason, Chaabane et al. [14] realized an experimental validation of their methodology for the design of frequency and environment "robust" UHF RFID Tags in an anechoic chamber. Their methodology [14] proposes an automated process of antenna generation mainly associated with a Genetic Algorithm optimizer using an RFID characterization monostatic method. The measurement setup is composed of a Vector Signal Generator (VSG; Agilent MXG-N5182A) used as transmitter, a Spectrum Analyzer (Tektronix RSA3408A) used as receiver, a Double Ridge Guide Horn with 7 dBi of gain and a circulator in order to isolate the transmission and reception channels. The VSG allows the emulation of any RFID commands [14].

Salas-Natera et al. [15] realized extensive measurement series in an anechoic chamber for complete calibration and characterization of active antenna arrays. Thanks to the automated system they were capable to measure any active antenna array with significant time and cost savings by connection the control system of the antenna under test to the anechoic chamber [15].

Shielded box to measure the sensitivity and directional characteristics of RFID tags employs two basic shielding components. The first component is the tetrahedral absorbers to limit multipath propagation of electromagnetic waves inside the box. The second component provides basic electromagnetic shielding. Electromagnetic Shielding Effectiveness (ESE) is a parameter, which describes an ability of specific material to limit a penetration of high frequency signal over certain barrier. Due to shielding that is applied to enclosures to isolate electrical devices from the 'outside world'. This component consists of the required thick value of duralumin sheet, which however leads to an increase in overall weight of anechoic chamber. In the case of a requirement to reduce the weight of the device, it could be possible to use lightweight construction thanks to any electrically conductive fabrics shielding electromagnetic fields - not only in the 868 MHz band [16]. For these materials, the size of ESE is possible to program before its production, and it is possible to use even more simulation methods and models [17].

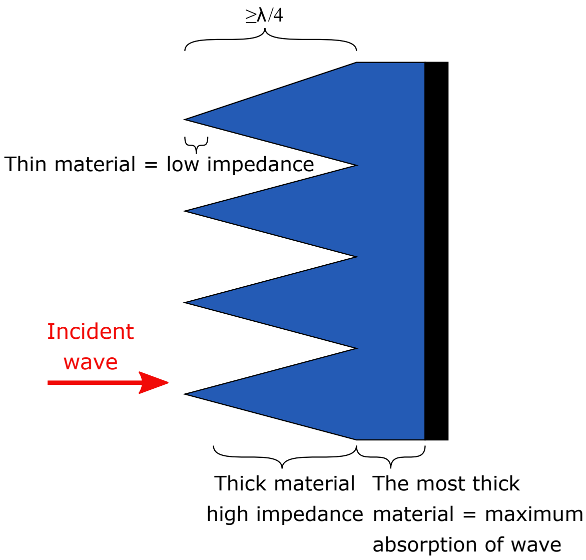

Fig. 1: Shape of electromagnetic absorbent material.

Absorbent materials for lining of anechoic chambers walls convert energy of incident wave into heat using either dielectric or magnetic loss. Currently, the dielectric materials are the most popular because the magnetic materials are too heavy and expensive [13].

The most common way of realizing broadband absorbent tiles as well as longitudinally inhomogeneous lossy environment is shown in Fig. 1.

Lining absorption elements have the shape of pyramids and cones made of polystyrene or polyurethane with graphite saturation. Linearly expanding cross section of the pyramids is implemented by the impedance transformer which anechoically converts the free space impedance at the tips of the pyramids into a very low impedance of the space completely filled with an absorber at the rear of the pyramids. Likewise, the absorbent tile (lines) losses gradually increase so the maximum energy absorption of the incident wave occurs only at the rear (the thickest part) portion of the absorber. Anechoic properties of the input of the entire absorbent lining are sometimes further improved by the fact that the tips of the pyramids have less graphite saturation (and therefore decreased losses) than their wide rears.

The pyramidal structure of the absorber, shown in Fig. 1, offers another advantageous feature. As shown in Fig. 2, when the wave is incident on the absorbent lining, it enters between the individual absorbent pyramids and is partially reflected on their surface.

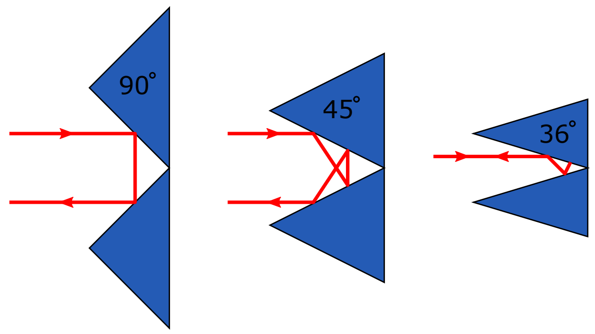

Fig. 2: Reflections in a pyramidal absorber.

Due to the pyramids bevel, these reflected waves are not returned directly into the interior of the chamber but they are directed into the neighbouring pyramid. They are partially reflected here again and the whole process is repeated. The reflected wave is returned to the interior of the chamber only after several partial reflections from the absorbent pyramids. Since with each reflection a portion of the wave energy is absorbed and only a portion is reflected, the total energy of the reflected wave after multiple reflections is considerably smaller. The anechoic absorption chambers (halls) nowadays represent nearly ideal measuring and testing space in the current EMC technology [13].

3.2. Determination of Minimum Reading Distance from the Antenna

Minimum distance of the object marked with RFID tag from the antenna should be equal or greater than 1.5 times the wavelength of the lowest frequency to be tested [18] and [19].

$$l = 1.5 \cdot \lambda, \tag{1}$$

$$\lambda = \frac{v}{f}, \tag{2}$$

where λ is wavelength, l is distance from the antenna, v is velocity of light and f is frequency.

$$\lambda = \frac{299\,792\,458}{865\,600\,000} = 0.35 \quad (\text{m}), \tag{3}$$

$$l = 1.5 \cdot 0.35 = 0.525 \quad (\text{m}). \tag{4}$$

Since the minimum distance should be equal or greater than the result of Eq. (4), the rotating platform was positioned 0.68 meters from the antenna.

4. HW Components

The chamber with dimensions of 80 cm × 80 cm × 150 cm is made of 3 mm welded aluminium sheet and to facilitate the operation it is positioned on the base 1 meter above ground. The base of the chamber is equipped with castors for easy handling. The inner surface of the chamber is equipped with two types of RF absorbing materials. There is foam absorber PXB-J500 with attenuation of 35 dB in the area of the most intense radiation of the reader antenna and PXB-J100 with attenuation of 17 dB on the other walls, to save space inside of the compact chamber. The chamber is equipped with a rotating platform for effective positioning of the examined object marked with tag in the full range of 360°.

Fig. 3: RFID reader Nebla.

Reading of RFID tags placed inside the chamber is provided by reader Nebla 402 equipped with antenna AKRC765. Nebla 402 operates in the frequency band 865.6–867.6 MHz, the area allowed by the European standard ETSI EN302-208-1 V1.3.1. (European Telecommunications Standards Institute). Maximum reader power is 33 dBm and its maximum sensitivity is −75 dBm. Nebla uses EPC global UHF (Ultra High Frequency) class1 Gen 2 and ISO 18000-6C protocol for communication with RFID tags. The reader can be connected via SMA (SubMiniature version A) connectors with up to 4 antennas. Nebla is connected to the network through the 10/100BASE-T Ethernet interface and the control software communicates with the reader via the protocol LLRP (Low Level Reader Protocol) V1.1., extended with additional XML (Extensible Markup Language) messages used to set the parameters of automatic platform rotation up.

The single-port antenna Kupson AKRC765 provides maximum performance and flexibility and is intended for the European zone ETSI EN302-208-1 V1.3.1. As

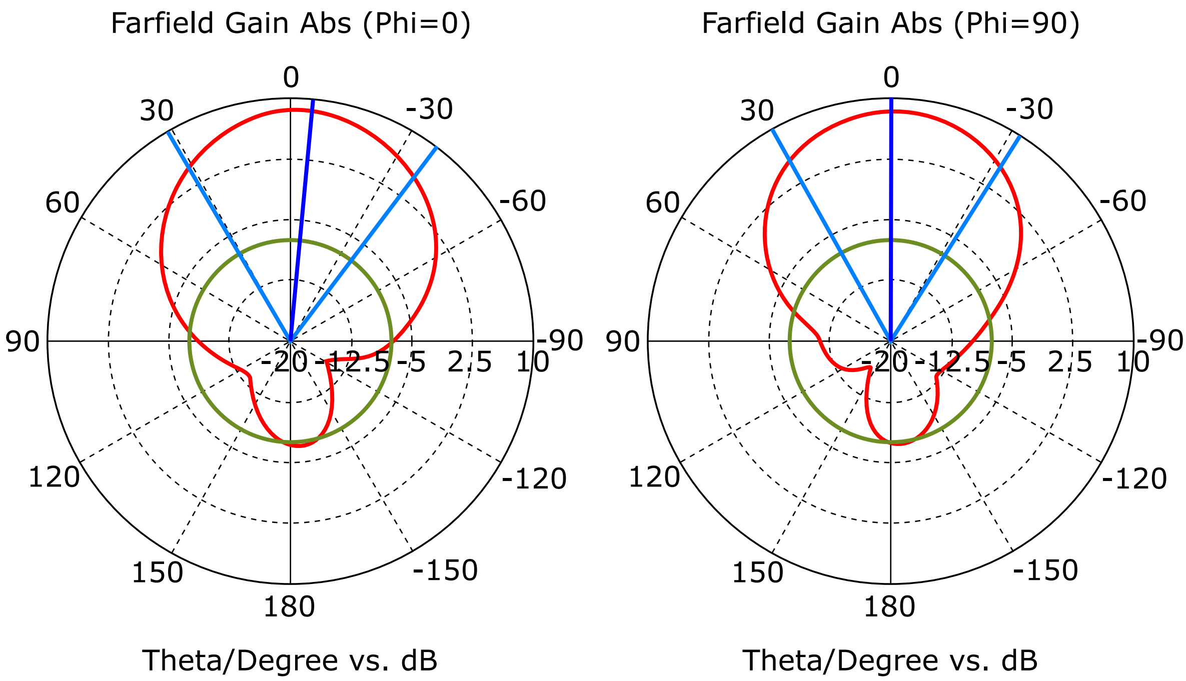

Fig. 4: Directional characteristics in the plane E and H.

can be seen in directional characteristics, Fig. 4, the radiation angle is 65° in both planes, E and H.

The antenna has a circular polarization and high gain which increases the reading range. Due to the low voltage factor of standing waves it reduces power losses in the reader. The antenna is protected against weather influence by a plastic high frequency transparent cover. Therefore, it can be installed in any part of the business environment, in the production halls, and warehouses or in any input receiving application.

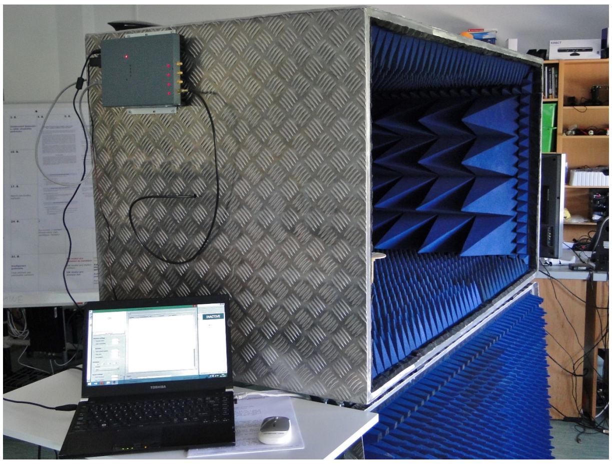

Fig. 5: RFID measurement chamber.

RFID antenna parametters:

- Frequency band: 865–868 MHz.
- Gain: 7 dBi.
- Radiation angle in H-plane: 65°.
- Radiation angle in E-plane: 65°.
- Suppression of unwanted emissions: > 15.
- Axial ration: < 2.
- Nominal impedance: 50 Ω.
- Resistance detection resistor: 10000 Ω.
- Coaxial connector: SMA(f).
- Polarization: RHCP.
- Maximum power: 10 W.
- Dimensions: 260 × 260 × 35 mm.
- The level of coverage: IP 54.
- Vibration resistance: IEC-68.
- Temperature range: -20 to $+55$ °C.

Rotation of the rotating platform is provided by servomotor Dynamixel MX-28 (Fig. 6) produced by company Robotis cooperating with the control system of the reader. The servomotor is equipped with a 12-bit encoder operating at 360° range (maximum theoretical resolution of 0.088°) equipped with a PID (Proportional-Integral-Derivative) controller. For our purpose, we use only the accuracy of one angular degree. Stall torque of the motor is 2.5 N at 12 V with idle speed of 55 RPM.

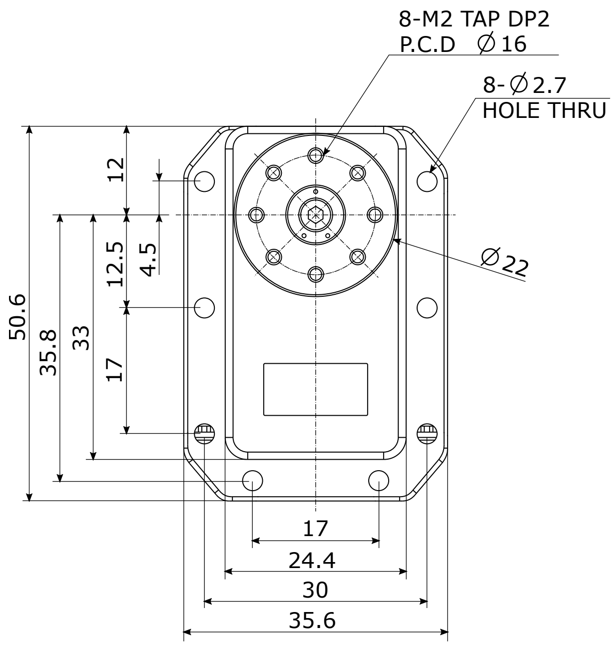

Fig. 6: Dynamixel MX-28 [17].

Connection of the servomotor and the control system of RFID reader is implemented using TTL (Transistor-Transistor-Logic) Level Multi Drop Bus in the form of Half-duplex Asynchronous Serial Communication. The control system of reader controls the motor through changes to the data in the control table with so-called Instruction Packet. For our application, the most important thing is setting of the specific position of the revolving platform in which we set the examined object marked with RFID tag. Implementation of platform positon regulation is realized with the PID controller pictured in the Fig. 7.

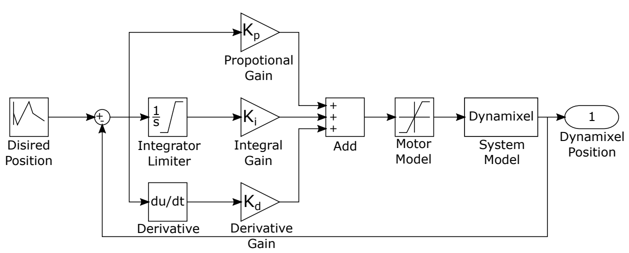

Fig. 7: Diagram of rotation regulation in MX-28 [17].

MX series will use the PID controller as a main control method. P gain refers to the value of proportional band. I_{gain} refers to the value of integral action. D_{gain} refers to the value of derivative action. Gains values are in between 0–254 [20].

$$k_p = \frac{P_{gain}}{8}, \tag{5}$$

$$k_I = \frac{I_{gain} \cdot 1000}{2048}, \tag{6}$$

$$k_D = \frac{D_{gain} \cdot 4}{1000}. \tag{7}$$

The PID controller is used because the integral control action eliminates bias offset. The important effect of the derivative term is that it gives a sharp response to suddenly changing signals [21].

5. Communication Protocol

Based on the analysis of communication standards of the best-selling UHF RFID readers, it was decided to use the LLRP standard [22] defined by the GS1 organization in the EPC Architecture of the Framework System EPC Global.

LLRP specifies interface between RFID readers and their connected client applications. The above mentioned protocol is called "low level reader protocol" (protocol on the low level). It provides full control of RFID devices, including continuity of commands used in the "air protocol" which is used for communication between the reader and the individual RFID tags. LLRP enables setting of the parameters and time constants of reading in accordance with the principles of "air protocol". LLRP respects and allows fulfilling of the requirements with possibility of detailed reader settings in physical layer of communication with regard to minimization of interference and optimization of the reading process with respect to the surrounding environment.

According [22], LLRP runtime operation consists of the following phases of execution:

- Capability discovery.
- Device configuration.
- [optional] Inventory and access operations setup.
- Inventory cycles executed - if tag conditions matched, access operations will be executed during inventory cycle execution. Access operations include reading, writing, and locking tag memory, killing tags, etc.
- RF Survey operations executed.
- Reports returned to the Client.

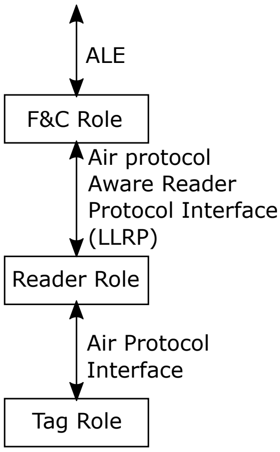

Fig. 8: Diagram of connection of LLRP to reading system.

A typical timeline of both LLRP and air protocol interactions between a client, reader, and population of tags is depicted in Fig. 9.

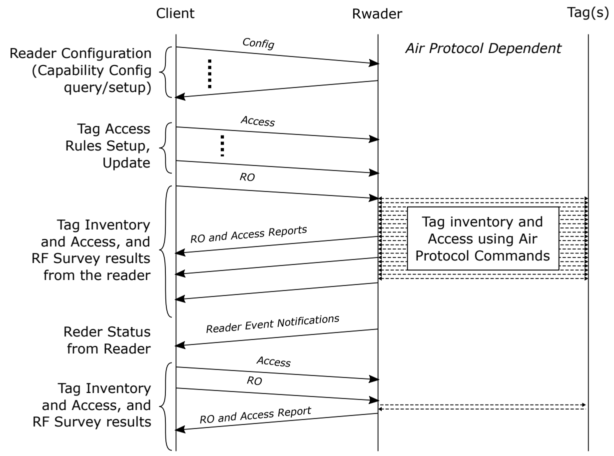

Fig. 9: Process of calibrating RFID reader and receiving information about reading in LLRP [22].

6. SW Application

The system for measuring of the margin power test consists of an anechoic chamber, where the RFID tag is placed on rotating platform, antenna, the device which rotates with rotating platform, UHF RFID reader, and application that implements the measurement control and interface. The situation is illustrated in Fig. 10.

The RFID reader is equipped with rotating platform motor controlling module for measurements, and common LLRP Protocol is extended by 2 custom commands: KUPSON_GET_MOTOR and KUPSON_SET_MOTOR. Position of rotation is controlled by PID controller as it was mentioned above.

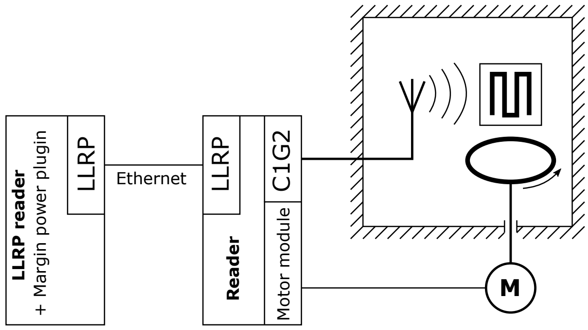

Fig. 10: Diagram of system for Margin power test measuring.

6.1. Application Structure

Measurements are essentially as follows: Application ensures gradual rotation of the rotating platform in predefined steps. The parameters TagSeen and RSSI (Received Signal Strength Indicator) are recorded at each step (rotation angle of the tag). During these steps the transmit power is increased step by step. The measurement can be performed repeatedly and automatically.

Measuring algorithm consists of a machine state that provides control of RFID reader and engine, and collects measured data. The measurement process consists of the following states, as shown at Fig. 11.

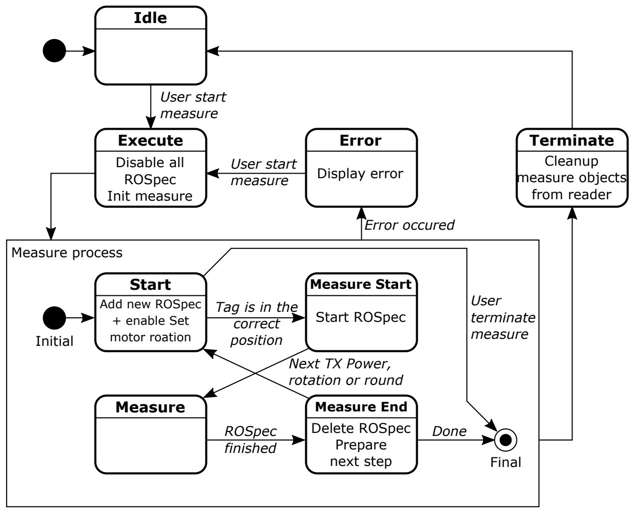

Fig. 11: State machine.

- Idle - Measuring not working. The user can set measurement parameters and launch the measuring in this state. The machine goes to "Execute" state by launching.
- Execute - application closes down all ROSpec of reader and initializes measuring process.

- Start - the ROSpec of measurement is designed in this step according to set parameters and uploaded to the reader. ROSpec has set StartTrigger to Null and StopTrigger to Duration, i.e. the length of measurement. ROSpec is loaded into the reader; it is authorized and instructed to rotate with rotating platform.
- MeasureStart - the correct rotation of rotating platform is checked in this step and if the rotation is done the ROSpec is launched.
- Measure - the measuring takes place during this step. After expiring the set time of measuring, the reader deactivates ROSpec and sends a notification to application. Application responds by going into "MeasureEnd" state.
- MeasureEnd - the ROSpec is deleted from reader and the transmit power is set for the next measurement. If the measurement has already taken place in its maximum transmit power, it proceeds to the next angle of measurement. The entire measurement is subsequently repeated. When the set number of repetitions is reached, the application goes to the "Terminate" state.
- Terminate - the machines remove all object associated with measuring and the measuring is closed.

To ensure sufficient measurement accuracy, the application provides in advance all communication and configuration specifications of reader and the actual measurement is initiated after that by sending a short message START_ROSPEC. Despite this, the application cannot ensure the exact duration between measurements. However, the length of the measurement is accurate because it is measured by the reader.

The application generates unique ID (ROSpecID) for each ROSpec during measuring. After reading the tag, the reader sends data in the message RO_ACCESS_REPORT about tag readings to the application. The application assigns a tag to the ROSpec according the ROSpecID and thus to a correct measurement step. If the defined step does not already contain the tag (paired according EPC - Electronic Product Code), it is added to the list of measurements as a new record. Otherwise, the data is aggregated (RSSI TagSeen accumulated and averaged). The entire procedure of receiving data of tags is shown in Fig. 12.

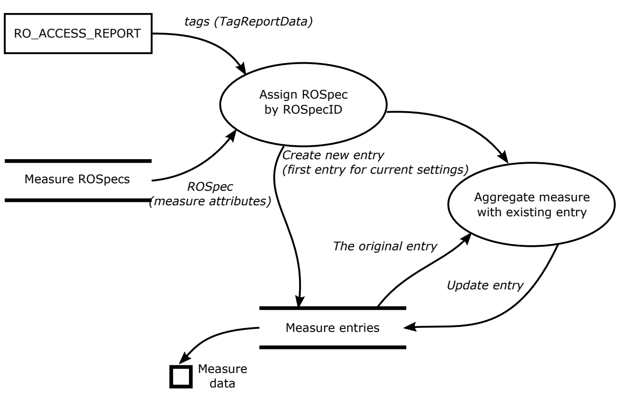

Fig. 12: Dataflow diagram.

Measurements are always bound to a specific antenna, although it is typically measured with only a single antenna.

In the following figure, Fig. 13, you can see the window of application where the measurement settings are defined. User can select how many times the measurements should be repeated (Rounds count). He may also sets the Inter-round time, which is the time when the reader is switched off between measurements, etc.

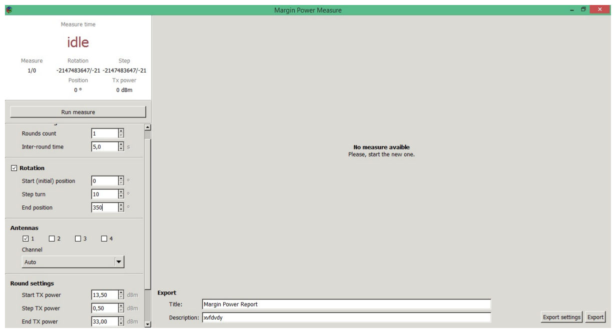

Fig. 13: SW application.

After setting all the variables, user just clicks on the Round Measure, triggering the start of measurement.

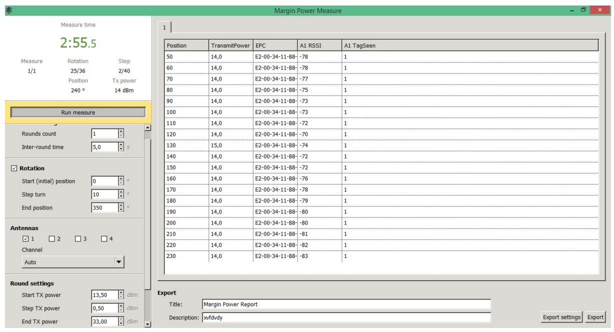

Fig. 14: SW application - measuring.

During the measurement, there is an overview about the time during which the measurement is taken, the current position, the current step, and so on.

After finishing the measurement, it is possible to export the report of measurements in csv format. The description of the measurement can be added to the Description field, for example information about object of measurement and used RFID tag type.

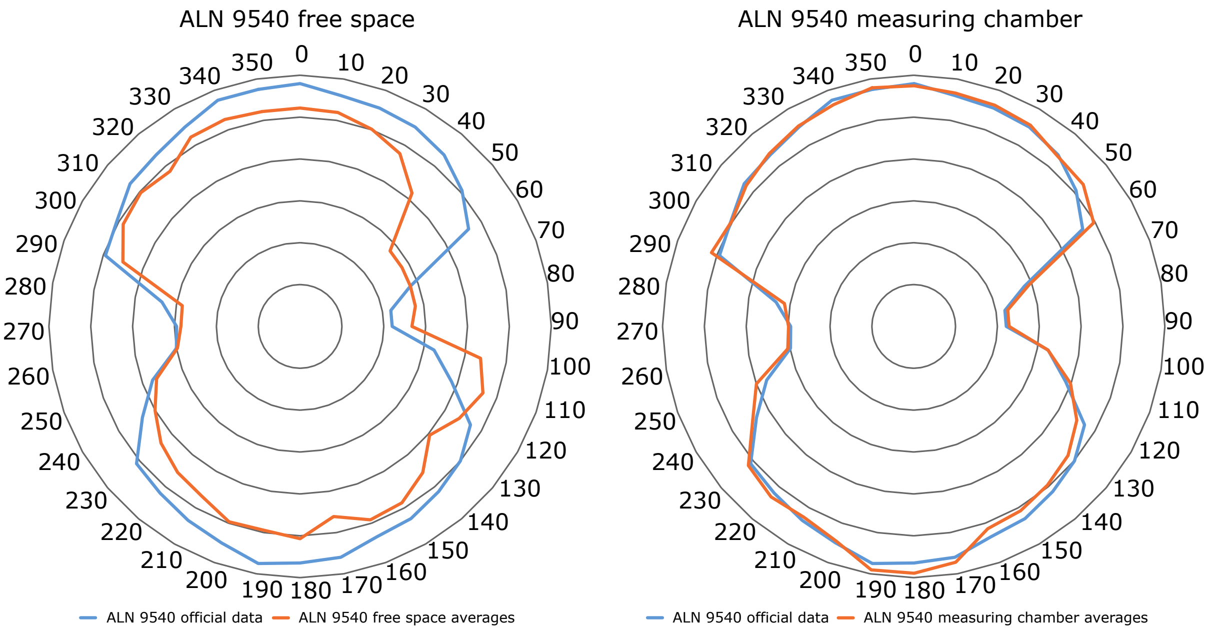

(a) Free space.

(b) Measuring chamber.

Fig. 15: Comparison of orientation sensitivity of tag ALN 9540 (datasheet vs. a) manual measuring and b) automatic chamber).

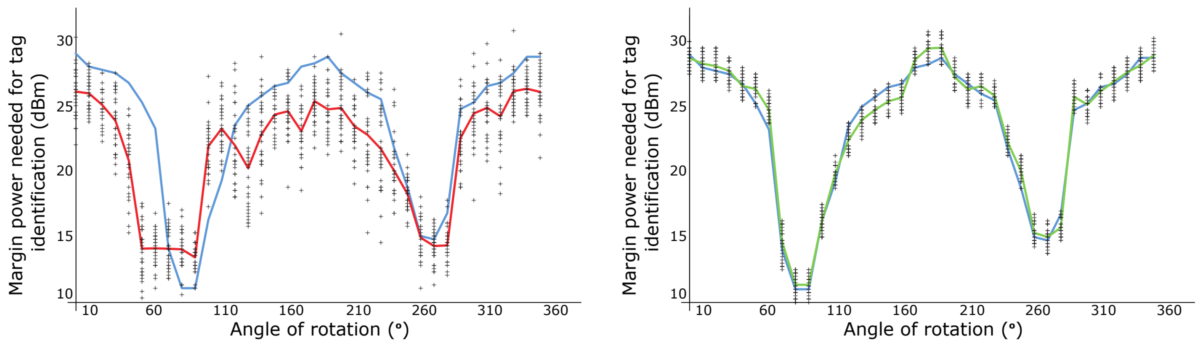

(a) Free space.

(b) Measuring chamber.

Fig. 16: Comparison measurement ALN 9540 official datasheet (blue) vs. a) manual measuring in free space (black measurements + red average) and b) automatic measuring in chamber (black measurements + green average)).

7. Empirical Evaluation and Results of Experiments

The RFID tag angular signal displacement towards the reader antenna can have a significant effect on tags reading properties. For this reason, we have performed an investigation of the directional characteristic based on the RFID tag angular displacement towards the antenna.

The purpose of this experiments was to evaluate functionality of developed automate measurement system and compare the orientation sensitivity characteristics with information listed in datasheets of selected RFID tags as well as with the characteristic obtained by manual measuring method in free space. Two RFID tags were used for this experiment:

- ALN 9540.
- Frog 3D.

The selected RFID tags have antennas in various forms. Frog 3D utilizes the option of double dipole offered by the Monza 4 chip [23], while ALN 9540 have a simple (however meandered) dipole antenna.

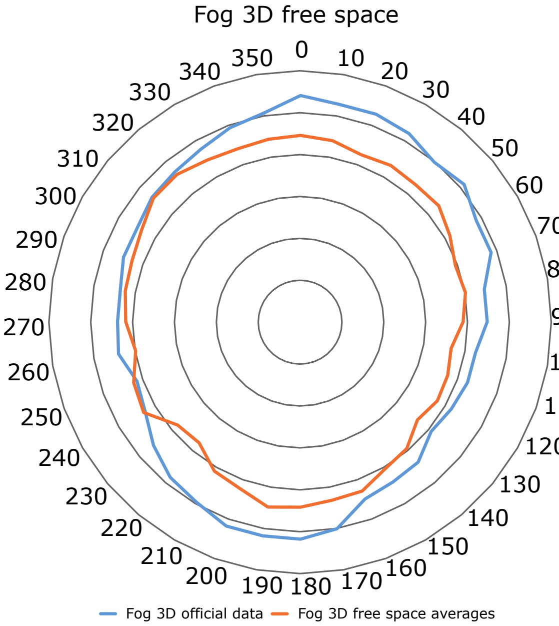

(a) Free space.

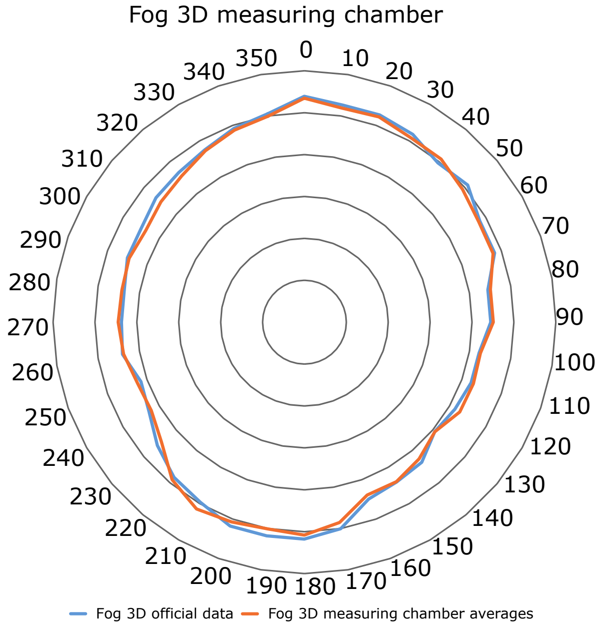

(b) Chamber.

Fig. 17: Comparison of orientation sensitivity of tag ALN 9540 (datasheet vs. a) manual measuring and b) automatic chamber).

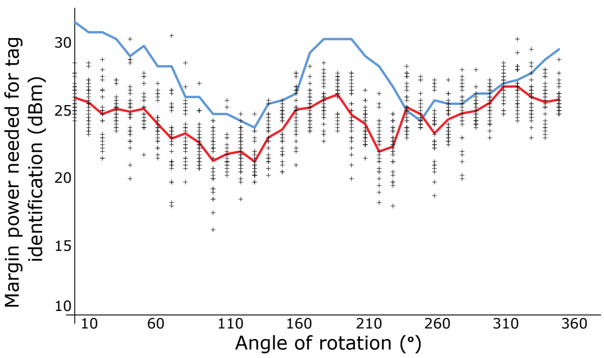

(a) Free space.

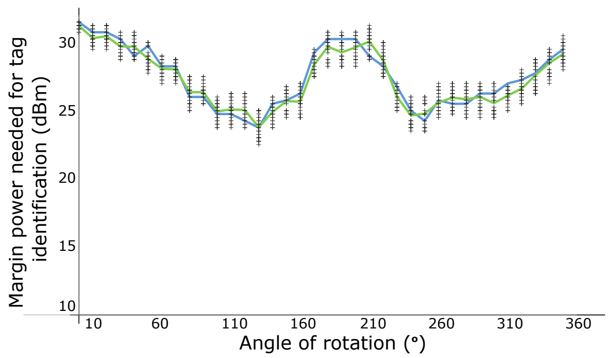

(b) Chamber.

Fig. 18: Comparison of orientation sensitivity of tag Frog 3D official datasheet (blue) vs. a) manual measuring in free space (black measurements + red average) and b) automatic measuring in chamber (black measurements + green average)).

RFID tag ALN 9540 parameters:

- Antenna dimensions: 94.8 × 8.1 mm.
- Frequency: 840–960 MHz.
- Chip: Alien Higgs-2.
- Protocol: ISO/IEC 18000-6C & EPCglobal Class 1 Gen 2.
- Memory: 96 bits EPC.
- Operating temperature: −20 to +93 °C.

RoHS Designed to comply with EU Directive 2002/95/EC RFID tag Frog 3D parameters:

- Antenna dimensions: 53 × 53 mm.
- Frequency: 860–960 MHz.
- Chip: Impinj Monza 4.
- Protocol: ISO/IEC 18000-6C & EPCglobal Class 1 Gen 2.
- Memory: 496 bit EPC and 512 bit User.
- Operating temperature: −40 to +85 °C.

As it can be seen bellow in the directional characteristics graph, the manufacturer delivered specifications (blue line) can be considered as a classic half wave dipole distribution. As it can be seen, there is a significant difference between the manufacturer professionally obtained values (blue line) and the measurements performed in our lab in the free space without a measuring chamber.

The much higher deviations of the measurements performed in the free space could be caused by the dynamic environment changes in the form of walking people, moving object, or external sources of similar frequency signal distraction.

Contrary, the measurements performed with the automated measurements system offer much higher reliability considering the standard deviations of the measured values and also a small difference from the official measurements supplied by the producer [24].

The difference is also apparent in the Fig. 16(a), where it is possible to see all the 30 measurements for each positions that are depicted as black points (some of the points are overlaid). According to this graph, we may consider that the free space measurement is not very reliable due to the large deviations of the measurements from their average (red line) and also because of their declination from the official measurements.

Figure 16(b) shows comparison of measurements done in anechoic chamber compared to data obtained from RFID manufacturer. Black point indicates measured values for each position. When we compare measured data shown in Fig. 16(a) and Fig. 16(b), it could be seen that automated measurement is more accurate and corresponds to the values from datasheet.

As can be observed in previous figures, Fig. 16(a) and Fig. 16(b), values of transmitting power vary in the range of ±13.5 dBm from the value indicated in the datasheet in case of the manual measurement, while it is only ±2.5 dBm in the case of measurements in an automatic anechoic chamber.

The following figures illustrate measurements of orientation sensitivity for RFID tag Frog 3D.

Perhaps more visible differences were achieved in the case of RFID tag Frog 3D. The measurements performed with the automated measurements system offer much higher reliability than measurements performed in free space, see Fig. 17(a) and Fig. 17(b).

In the case of measuring in an anechoic chamber, when the absorbent material absorbs the reflected radiation, the results of measuring corresponds to the characteristics indicated by the manufacturer [25].

Figure 18(a) and Fig. 18(b) show comparison of measurements carried out in free space and in anechoic chamber compared to data obtained from RFID manufacturer. Values of transmitting power vary in the range of ±13.25 dBm from the value indicated in the datasheet in case of the manual measurement, while it is only ±1.75 dBm in the case of measurements in an automatic anechoic chamber.

8. Conclusion

The basic technological level of the Automatic Identification and Data Collection (AIDC) means utilization of HW components and product identification using RFID technology. Such information received from the process can be used further at higher levels of control.

The basic and necessary step to achieve the objective in the form of communicating and sharing information from separate parts of the logistics chains via the EPCIS and EPCglobal Network is to design a tag, the identifier of the item, i.e. using the automatic identification tools. Each object has its own specific properties and therefore it is necessary to find the best RFID tag before implementing RFID technology into practice. The developed device can help to make this process easier and more accurate.

The primary purpose of designing and creating an anechoic chamber was to achieve the highest possible repeatability and reproducibility of measurements.

The important part of this realization was to create and optimize software for UHF RFID reader Nebla, leading to a higher degree of automation of tests performed in the laboratory, and their easier statistical processing. The enhanced software allows us to create a transparent and clear outcomes and results presented in a comprehensible and understandable form.

As was demonstrated in this paper, the developed solution achieves highly accurate results compared to data obtained by measuring in free space. Even the results are not equal; it is possible to assume that there is a strong correlation with data listed in datasheets.

This system leads to significant time savings and improve all measurements with RFID technology. The proposed solution gives an extra tool for implementing the automatic identification technology. Such a tool will save them a lot of time and costs associated with implementation of measurement, including labor costs. Results of the developed solutions reflect current problems but are also targeting several years into the future, when the use of RFID will become more accentuated in accordance with the indicia of the framework of EU programs and the experimental verification will be therefore required more often. Measurements described in this paper proved the real usability of our developed chamber for the measuring of marked objects and items.

The proposed solution has already found a series of clients from the industrial sector, who want to find the directional characteristics and the ability to read RFID tag placed on that particular product in the anechoic chamber. About 90 % of them intend to order measurement in the future. Regarding other potential users, 68 % from surveyed companies expressed for the possibility that they will use this service in the future, 24 % do not know at the moment, and only 8 % see no reason to use this chamber for their needs.

Acknowledgment

This contribution was supported by the Moravian-Silesian Region in the subsidy title no. 1. Grant program supports business in the Moravian-Silesian Region, 2014.

This contribution was supported by the Ministry of Education, Youth and Sport as a part of an Inter-Eureka international project titled "Auto-ID technology and the Internet of Things to enhance the quality of health services" - identification number LTE117005, international project code: E!11158 U Health.

References

[1] LIL, B., Y. HE, L. ZUO and Y. LONG. Metric of the Application Environment Impact to the Passive UHF RFID System. *IEEE Transaction o Instrumentation and Measurement.* 2014, vol. 63, no. 10, pp. 2387–2395. ISSN 1557-9662. DOI: 10.1109/TIM.2013.2287119.

[2] LEE, Y.-H., M.-Y. TSAI, C.-F. YANG and I. LIN. A 3D RFID Static Test System Using a Spherical Near-Field Antenna Measurement Chamber. *IEEE Transaction on Instrumentation and Measurement.* 2012, vol. 61, no. 1, pp. 362–370. ISSN 1558-2221. DOI: 10.1109/TAP.2012.2216493.

[3] BETTA, G., D. CAPRIGLIONE, L. FERRIGNO and G. MIELE. Influence of Wi-Fi Computer Interfaces on Measurement Apparatuses. *IEEE Transaction o Instrumentation and Measurement.* 2010, vol. 59, no. 12, pp. 3244–3252. ISSN 1557-9662. DOI: 10.1109/TIM.2010.2047303.

[4] RFID Testing. In: *National Instruments* [online]. 2017. Available at: `http://sine.ni.com/ind-app/app/app/p/id/app-63/lang/cs`.

[5] NIKITIN, P. V. and K. V. S. RAO. LabVIEW-Based UHF RFID Tag Test and Measurement System. *IEEE Transactions on Industrial Electronics.* 2009, vol. 56, no. 7, pp. 2374–2381. ISSN 0278-0046. DOI: 10.1109/TIE.2009.2018434.

[6] RFID Measurement Solutions. In: *Voyantic* [online]. 2017. Available at: `http://voyantic.com/products/tagformance-pro`.

[7] NIKITIN, P. V., K. V. S. RAO and S. LAM. UHF RFID tag characterization: Overview and state-of-the-art. In: *Everett* [online]. 2012. Available at: `http://citeseerx.ist.psu.edu/viewdoc/download?doi=10.1.1.362.2900&rep=rep1&type=pdf`.

[8] COLELLA, R., L. CATARINUCCI, P. COPPOLA and L. TARRICONE. Measurement Platform for Electromagnetic Characterization and Performance Evaluation of UHF RFID Tags. *IEEE Transactions on Instrumentation and Measurement.* 2016, vol. 65, iss. 4, pp. 905–914. ISSN 0018-9456. DOI: 10.1109/TIM.2016.2516322.

[9] RAO, K. V. S., P. V. NIKITIN and S. LAM. Antenna Design for UHF RFID Tags: A Review and a Practical Application. *IEEE Transactions on Antennas and propagation.* 2005, vol. 53, no. 12, pp. 3870–3876. ISSN 1558-2221. DOI: 10.1109/TAP.2005.859919.

[10] COSTA, L. R. M. UHF RFID tags in a controlled environment: Anechoic chamber case. In: *2015 IEEE Brasil RFID.* Sao Paulo: IEEE, 2015, pp. 23–27. ISBN 978-1-5090-1068-4. DOI: 10.1109/BrasilRFID.2015.7523836.

[11] LUZ, A. and F. COSTALONGA. RFID Tag Tests: comparison between GTEM cell and anechoic chamber results. In: *2014 IEEE Brasil RFID.* Sao Paulo: IEEE, 2014, pp. 50–53. ISBN 978-1-4799-7045-2. DOI: 10.1109/BrasilRFID.2014.7128964.

[12] FELIX, M., F. PEREIRA, V. FERRO, E. MARTINS and I. DINIZ. Using labview to automate RFID tag tests: Comparison between implemented system and voyantic test system. In: *2015 IEEE Brasil RFID.* Sao Paulo: IEEE, 2015, pp. 5–9. ISBN 978-1-5090-1068-4. DOI: 10.1109/BrasilRFID.2015.7523832.

[13] PAUL, C. R. *Introduction to electromagnetic compatibility.* New Jersey: John Wiley & Sons, Inc., 2006. ISBN 978-0-471-75500-5.

[14] CHAABANE, H., E. PERRET and S. TEDJINI. A Methodology for the Design of Frequency and Environment Robust UHF RFID Tags. *IEEE Transactions on Antennas and Propagation.* 2011, vol. 59, no. 9, pp. 3436–3441. ISSN 1558-2221. DOI: 10.1109/TAP.2011.2161556.

[15] SALAS-NATERA, M. A., R. M. RODRIGUEZ-OSORIO and L. DE HARO. Procedure for Measurement, Characterization, and Calibration of Active Antenna Arrays. *IEEE Transactions on Instrumentation and Measurement.* 2013,

vol. 62, no. 2, pp. 377–391. ISSN 1557-9662. DOI: 10.1109/TIM.2012.2217662.

[16] VOJTECH, L. and M. NERUDA. Application of Shielding Textiles for Increasing Safety Airborne Systems - Limitation of GSM Interference. In: *The Ninth International Conference on Networks*. Los Alamitos: IEEE, 2010, pp. 157–161. ISBN 978-1-4244-6083-0. DOI: 10.1109/ICN.2010.35.

[17] LOPEZ, A., L. VOJTECH and M. NERUDA. Comparison among Models to Estimate the Shielding Effectiveness Applied to Conductive Textiles. *Advances in Electrical and Electronic Engineering*. 2013, vol. 11, no. 5, pp. 387–391. ISSN 1336-1376. DOI: 10.15598/aeee.v11i5.902.

[18] DOBKIN, D. M. *The RF in RFID: passive UHF RFID in practice*. 1st ed. Amsterdam: Elsevier Inc./Newnes, 2008. ISBN 978-0-750-68209-1.

[19] HUNT, D. V., A. PUGLIA and M. PUGLIA. RFID: *A Guide to Radio Frequency Identification*. 1st ed. New Jersey: John Wiley and Sons, 2007. ISBN 978-0-470-10764-5.

[20] MX-28T/MX-28R. ROBOTIS e-Manual v1.27.00. In: *Robotis* [online]. 2010. Available at: http://support.robotis.com/en/.

[21] FRANKLIN, G. F., J. POWELL and A. EMAMI-NAEINI. *Feedback control of dynamic systems*. 1st ed. New Jersey: Pearson/Prentice Hall, 2010. ISBN 978-0-136-01969-5

[22] Low Level Reader Protocol (LLRP), Version 1.1. In: *EPCGlobal* [online]. 2010. Available at: http://www.gs1.org/sites/default/files/docs/epc/llrp_1_1-standard-20101013.pdf.

[23] Inc. Monza 4 Tag Chip Datasheet. In: *Impinj* [online]. 2015. Available at: https://support.impinj.com/hc/en-us/article_attachments/201102327/Monza_4_Tag_Chip_Datasheet_20150120_R8.pdf.

[24] ALN-9540 Squiggle Inlay. In: *Alien Technology* [online]. 2008. Available at: http://www.falkensecurenetworks.com/PDFs/DS_ALN_9540_Squiggle_tag.pdf.

[25] Frog 3D. In: *Smartrac* [online]. 2017. Available at: https://www.smartrac-group.com/files/content/Products_Services/PDF/0011_SMARTRAC_FROG_3D_2in.pdf.

About Authors

Pavel STASA was born in Ostrava. He finished his doctoral studies in 2012 and he focuses his on modelling and simulation of flow using Fluent SW. He spent one semester at Dongguk University in Seoul, it was focused on RFID technology. His research area is modelling and simulation of flow using CFD program Fluent, RFID, NFC technology and IoT. Since 2015 he has been a head of RFID laboratory at VSB–Technical University of Ostrava.

Jiri SVUB was born in Uherske Hradiste. He has 7-year experience with scientific work on projects at the ILAB RFID. His experience covers fields of automation, AutoID, technical equipment. His abilities include, above all, system analysis, analysis and design of HW and SW equipment, lab testing and experiments with RFID technology, statistic data processing, research of RFID potential in perspective fields.

Filip BENES was born in Bohumin. He received Ph.D. in 2012, his thesis was focused on RFID in retail. He has 7-year experience with research work on projects at the ILAB RFID. Experience in the fields of AutoID, Augmented Reality and IoT. His abilities include, above all, system analysis of a problem, testing, analysis, and design of HW and SW equipment, research of RFID potential in perspective fields.